Phase Behavior of New Side Chain Smectic C* Liquid Crystalline Block Copolymers

Wen Yue Zheng and Paula T. Hammond*

Department of Chemical Engineering, Massachusetts Institute of Technology, Cambridge, Massachusetts 02139

Received June 26, 1997; Revised Manuscript Received November 19, 1997

ABSTRACT: The liquid crystalline and microphase behavior of new chiral side chain liquid crystalline diblock copolymers is described. The materials, which contain a smectic C* mesogen, are block copolymers of polystyrene and methacrylates containing (s)-2-methyl-1-butyl-4′-(((4-hydroxyphenyl)carbonyl)oxy)-1,1′-biphenyl-4-carboxylate mesogens. The influences of the liquid crystalline (LC) mesophase on block copolymer ordering and of the block copolymer morphology on LC properties as a function of molecular weight and block copolymer composition are discussed. Microphase segregated structures were observed for blcok copolymers ranging from 24 to 63% w/w LC block. The lamellar domains of the block copolymers stabilize the layered smectic mesophase, particularly the smectic C* phase. The length of the polystyrene block, as well as the LC block, affected LC phase transition temperatures, probably due to phase mixing and the nature of the block copolymer interface. When the molecular weight is low, and the liquid crystal block content is high, the order−disorder transition temperature, at which block copolymer phase segregation is observed, and the LC clearing point occur at the same temperature; this correlation between LC order and the ODT has not been reported before for LC side chain block copolymers. The block copolymer morphology in these cases is arranged to accommodate the focal conic superstructure seen in optical micrographs of this LC block copolymer.

Introduction

Side chain liquid crystalline polymers have been the subject of extensive investigation for several years.[1−13] Block and multiphase copolymers which contain side chain liquid crystalline segments may provide a new means of combining the advantages of traditional polymeric systems with liquid crystalline electro-optical properties. The microphase-segregated morphologies of these systems result in isolated domains of liquid crystalline polymer and glassy, amorphous polymer. The resulting materials can form free-standing films or uniform coatings which have mechanical properties ranging from that of a stiff glass to an elastomeric film.

The presence of phase morphology in these systems provides a new environs for liquid crystalline polymers, in which the order of the block or segmented copolymer morphology is superimposed on the liquid crystalline ordering. It is expected that the fraction of liquid crystalline segment, the molecular weight, degree of phase segregation, and ordering of domains using processing techniques will have significant effects on the final electro-optical properties. It is also anticipated that many of these materials may exhibit other interesting properties, such as mechano-optical and piezoelectric behavior. The wide range of morphologies and the self-assembling nature of block copolymers provide the opportunity to design materials for a variety of liquid crystalline applications by varying chemical structure and materials processing techniques.

Two new series of liquid crystalline (LC) diblock copolymers have been synthesized in our group and fully characterized; these materials are among the first monodisperse block copolymers which contain a side chain ferroelectric smectic C* mesogen;[9,14] a series of chiral C* polystyrene−polyisoprene based polymers have also been synthesized by Mao et al.[15] using polymer analogous substitution on an LC diblock copolymer, and poly(vinyl ether) block copolymers have been synthesized by Omenat et al. using direct living cationic polymerization of the mesogen.[11] The chiral smectic C* mesogen can potentially impart ferroelectric and piezoelectric properties to these polymers, forming the basis for a novel series of thermoplastic LC microphase polymers. In this paper, we address the basic liquid crystal phase behavior exhibited in polystyrene−polymethacrylate chiral LC block copolymers as a function of molecular weight and block copolymer composition, including the effect of phase-segregated morphology on the stabilization of the smectic C* phase. The relationships between liquid crystalline order, block copolymer morphology, and the order−disorder transition of the block copolymers are key to understanding how polymer structure may be altered to design new LC materials. In this paper we address the phase transitions observed in new well-defined smectic C* block copolymers, the relationship between liquid crystalline and block copolymer mesophase order. This series is particularly unique because its low to moderate molecular weight range and relative interaction between blocks has allowed us to observe systems with LC-induced order−disorder phase transitions for the first time. A separate paper will give a detailed account of morphology and orientation effects on morphology and structure in these materials.[16]

Experimental Section

Synthesis. Monomers, homopolymers, and block copolymers were synthesized with methods described in a previous paper.[9] All block copolymers were prepared by sequential anionic polymerization of styrene, followed by endcapping with diphenylethylene, and subsequent addition of the mesogenic methacrylate monomers. The molecular weight of the LC methacrylate block in most of the polymers synthesized with this approach ranged from 7000 to 9000 (Table 1). It has been shown that various types of lithium salts can be used in anionic polymerization of methacrylate monomers to dissociate the

S0024-9297(97)00940-6 CCC: $15.00
Published on Web 01/22/1998

Table 1. Summary of the Molecular Weight and Distribution, and Composition in Smectic C* Side Chain Liquid Crystalline Homopolymers and Diblock Copolymers

	$10^{-3}M_n$[a]			
polymers	PS Block	LC Block	M_w/M_n	LC content
PMHBPB		7.0	1.10	1.00
PS-HBPB51	6.8	7.7	1.07	0.515
PS-HBPB43	10.3	7.4	1.08	0.434
PS-HBPB41	11.0	7.3	1.06	0.414
PS-HBPB32	17.7	7.3	1.07	0.317
PS-HBPB24	40.3	7.7	1.12	0.244
PS-HBPB20	21.8	5.3	1.11	0.201
PS-HBPB12	48.1	4.8	1.08	0.120
PMDBPB		8.3	1.10	1.00
PS-DBPB63	5.7	8.7	1.09	0.627
PS-DBPB57	8.1	9.4	1.13	0.568
PS-DBPB49	10.3	8.7	1.11	0.491
PS-DBPB37	14.3	8.3	1.09	0.367
PS-HBPB49[b]	15.6	11.5	1.16	0.488
PS-DBPB59[b]	11.7	17.2	1.06	0.592
PS-DBPB45[b]	28.6	22.9	1.24	0.452

[a] Molecular weight was determined by GPC in toluene and THF eluents at 25 °C. [b] Block copolymers with high molecular weight were synthesized in the presence of LiCl salts as ligand.

aggregates formed by the propagating anionic species;[7] the presence of salts was found to affect not only the polydispersity but the chain length and living nature of propagation. To achieve samples with higher molecular weight LC blocks (>9000), LiCl (2.5×10^{-3} M) was introduced into the THF solvent before the addition of initiator. The LiCl (99.99%, Aldrich) was dried at 130 °C for 12 h prior to use in the reation. All polymers were purified by reprecipitation twice from THF to methanol and extensively dried in a vacuum oven before characterization.

Characterization. A Bruker MW 250 MHz proton NMR was used to verify the chemical structure of all polymers and determine the composition of each block. A Waters gel permeation chromatograph with 440 UV absorption detector and R401 differential refractometer was used to determine the molecular weights of the homopolymers; tetrahydrofuran and toluene were used as the mobile phases at 1.0 mL/min, and the Waters polystyrene gel columns were calibrated with monodisperse polystyrene standards. Polarizing optical microscopy was used to identify liquid crystalline phases using a Leitz optical microscope with CCD camera attachment and Mettler FP-82 hot stage and controller (heating/cooling rate of 10 °C/min). A Perkin-Elmer DSC-7 (differential scanning calorimeter) with a cooling accessory was used to determine the thermal transitions in the homopolymer and block copolymers synthesized (scanning rate of 20 °C/min). The WAXD (wide angle X-ray diffraction) measurements were performed with nickel-filtered Cu Kα radiation with a Rigaku 250 XRD diffractometer. Divergence slit (0.5), scattering slit (0.5), and receiving slit (0.15) were selected to detect the diffraction at small angles down to 1°.

The SAXS (small angle X-ray scattering) measurements were performed on a computer-controlled system consisting of a Rigaku rotating-anode Cu Kα X-ray source operating at 40 kV and 30 m and a Nicolet two-dimensional position-sensitive detector. The 2-D Siemens detector was placed at a distance of 130 cm from the sample. Data were obtained in the form of scattered X-ray intensity, I, as a function of the scattering vector $\mathbf{q} = (4\pi/\lambda) \sin \theta$ (nm^{-1}). Thin films were slowly cast from 3 wt % solution in toluene and dried in vacuum for 2 days to remove remaining solvent. The films were then annealed at 110 °C for 2 days before SAXS measurements or sample preparation for transmission electron microscopy (TEM). Temperature-controlled SAXS experiments were conducted on a self-designed sample holder consisting of two aluminum plates with a central hole and the Mettler FP-82 hot-stage and controller. An internal period of 10 min was used to anneal the sample to obtain equillibrium structure before data acquisition at each elevated temperature.

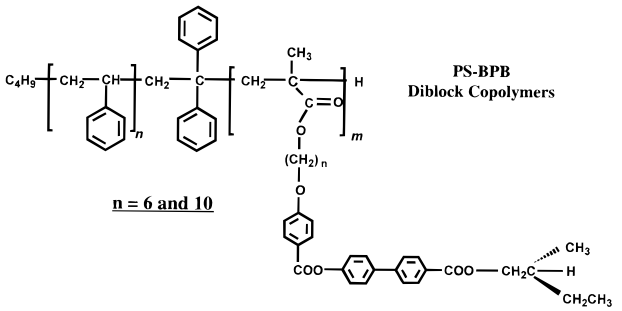

Figure 1. Chemical structures of PS-HBPB and PS-DBPB block copolymer series.

TEM thin sections (40−60 nm) were prepared by cutting a small piece of thin film embeded in epoxy resin on a Reichert-Jung FC4E Ultracut E microtome equipped with a diamond knife. The sections were collected on copper grids and were stained in RuO_4 vapor for 30 min to make enough phase contrast for TEM observation. The TEM morphology studies were carried out using a JEOL 200CX electron microscope in bright field mode operated at accelerating voltages of 200 kV.

Results and Discussion

Polymer Design and Structure. To address the range of material properties of interest, such as electro-optical behavior, the objective in designing the block copolymers was to obtain systems with a rigid, glassy block and a liquid crystalline block with a lower T_g. In this work, well-defined block copolymers were synthesized by the direct anionic polymerization of an LC mesogen. The use of this approach allowed us to maintain control of the block copolymer composition and the degree of substitution on the polymer backbone. Figure 1 contains the chemical structure of the BPB block copolymer series. The glassy block chosen for these materials was polystyrene, due to its ease of synthesis and high glass transition temperature. A methacrylate backbone was used based on previous studies indicating the successful direct anionic polymerization of nematic and smectic A methacrylate mesogens.[7,17] The mesogenic monomer (I) is a methyl methacrylate with a liquid crystalline side chain consisting of a rigid biphenyl benzoate core with a terminal chiral end group. The aromatic group is connected to the methacrylate with an alkyl spacer of either six (hexyl) or ten (decyl) methylene units. The alkyl group, which facilitates smectic layering in the block copolymers, also serves a second role in lowering the glass transition temperature of the methacrylate backbone. Block copolymers were synthesized using direct anionic polymerization of the methacrylate monomer from propagating polystyryl anion; complete details of the synthetic approach have been addressed in an earlier publication.[9] No evidence of side reaction was observed in NMR or gel permeation chromatography (GPC).

In general, the block copolymer composition was varied by increasing the size of the PS block and maintaining the LC block size constant. Higher molecular weight polymers with compositions ranging from 45 to 59 wt % liquid crystal were also synthesized for comparison with their lower molecular weight analogs; these high molecular weight polymers are indicated in the table with asterisks. By adjusting polymerization conditions such as solvent and the addition of Li salts, it is possible to use direct anionic polymerization of the biphenyl benzoate mesogens to obtain LC block polymers with up to 50 000 molecular weight. It has been

Table 2. Phase Transitions for Monomers, Homopolymers, and Diblock Copolymers

sample	treatment	phase transitions, °C (enthalpy change, J/g)[a]	morphology
MHBPB	heating	K 75 (64.2) S_C* 129 (2.2) S_A 138 (0.76) Ch 170 (0.72) I	
	cooling	I 153 (−0.52) Ch 133 (−0.49) S_A 125 (−0.74) S_C* 27 (−4.86) K	
PMHBPB	heating	G_{LC} 35 S_C* 120 S_D 137.1 (0.22) S_A 157 (3.41) Ch 170 I	
	cooling	I 150.3 (−1.05) S_A 127.0 (−0.10) S_C* 26.7 G_{LC}	
PS-HBPB51	heating	G_{LC} 24 S_C* Gs 89.3 S_C* 138 (0.20) S_A 167 Ch 172 (2.0) I	lamellar
	cooling	I 164 (−1.37) S_C* 87 Gs S_C*	
PS-HBPB43	heating	G_{LC} ~34 S_C* Gs 95.1 S_C* 136 S_A 158 Ch 177 (1.55) I	lamellar
	cooling	I 166 (0.56) S_C* 88 Gs S_C	
PS-HBPB40	heating	G_{LC} 33 Sc* Gs 97 Sc* 140 (0.87) S_A 172 (1.9) I	lamellar
	cooling	I 159 (0.36) Sc* Gs 91	
PS-HBPB32	heating	G_{LC} ~34 S_C Gs 98 S_C* 163 (0.50) S_A 181 (0.27) I	lamellar
	cooling	I 171 (−0.35) S_A 156[@] S_C* 87 Gs S_C*	
PS-HBPB24	heating	96 Gs ~180 I	disc. LC phase
	cooling	I ~160 Gs 87	
PS-HBPB12	heating	Gs 98	disc. LC phase
	cooling	Gs 88	
MDBPB	heating	Ks 15.6 (3.5) K 46.5 (37.8) S_C* 92.6 (0.55) S_A 115.8 (4.6) I	
	cooling	I 113.0 (−4.48) S_C* 14.5 (−16.8) K −8.2 (−7.2) Ks	
PMDBPB	heating	G_{LC} 18 S_C* 128 (0.71) S_A 140 Ch 146 (3.88) I	
	cooling	I 138 (−1.18) S_A 116[@] S_C* 12 G_{LC}	
PS-DBPB62	heating	G_{LC} 27 S_C* Gs 80 S_C* 145 (0.16) S_A ~154[@] Ch 160 (1.96) I	lamellar/HPL
	cooling	I 153 (−1.46) S_A 120[@] S_C* 86 Gs	
PS-DBPB57	heating	G_{LC} 26 S_C* Gs 87 S_C* 150 (0.14) S_A ~163[@] Ch 169 (1.07) I	lamellar
	cooling	I 159 (−0.84) Ch 120[@] S_C* 78 Gs	
PS-DBPB49	heating	G_{LC} 27 S_C* Gs 94 S_C* 163 (1.22) I	lamellar
	cooling	I 154 (−0.45) S_C* 85 Gs S_C	
PS-DBPB37	heating	G_{LC} 26 S_C* Gs 95 S_C* 167 (0.73) I	lamellar
	cooling	I 157 (−0.54) S_C* 87 Gs S_C* 27 G_{LC}	
PS-HBPB49*	heating	G_{LC} ~34 Gs 79 S_C* 138 S_A 165 I	lamellar
	cooling	I 154 S_C* 73 Gs	
PS-DBPB45	heating	G_{LC} 27 Gs 96 S_C* 135 (0.41) S_A 175 (2.58) I	lamellar
	cooling	I 161 (−1.02) S_C* 89 Gs	
PS-DBPB59*	heating	G_{LC} 29 Gs 86 S_C* 122 (1.05) S_A 181.4 (2.44) I	lamellar/HPL
	cooling	I 170 (−0.37) S_A 149 (−0.15) S_C* 76 Gs 6.1 G_{LC}	

[a] Most transitions determined by DSC runs at a scan rate of 20 °C/min and microscopy; G_{LC} Tg of LC segment; Gs gTg of polystyrene; @ transitions were determined by optical microscope alone. HPL: hexagonal perforated layered morphology.

difficult to obtain such high molecular weights using a direct polymerization approach with the biphenyl benzoate mesogens.[9] These findings suggest that, under the appropriate polymerization conditions, fairly large molecular weights can be obtained with a living polymerization, while maintaining 100% substitution of the polymer backbone. This factor is important in ultimately gaining complete control of the degree of substitution along the backbone as well as the polydispersity.

Liquid Crystalline Characterization. DSC and polarizing optical microscopy were used to identify liquid crystalline phases in the homopolymers and diblock copolymers. WAXD was also used to verify the presence and nature of the observed smectic phases and the smectic layer spacings. The results of these investigations are summarized in Table 2, which lists the liquid crystalline transitions observed for each polymer. In this section, the detailed chararacterization of a typical block copolymer from each series is presented as well, to give an idea of the overall LC behavior observed in these materials.

Figure 2 contains a DSC thermogram of a typical hexyl series block copolymer, PS-HBPB51, with corresponding optical micrographs. The glass transition temperature of the liquid crystalline block was generally difficult to detect for this block copolymer series and could only be seen after quenching the sample from the isotropic state. Above the LC block glass transition, a birefringent smectic texture was typically observed. The liquid crystalline texture would brighten, and become more mobile above the T_g of the polystyrene block. Some of the block copolymers exhibited a fairly narrow temperature range of cholesteric texture prior to isotropization, as shown for PS-HBPB51 at 167 °C. Figure 3 illustrates the DSC and corresponding optical microscopy of the decyl spacer block copolymer, PS-DBPB57, which has a longer, decyl spacer group attaching the mesogen to the methacrylate main chain. The glass transition temperatures of both blocks is evident in this thermogram; the decyl series polymers usually exhibited more well-defined thermal transitions and optical textures than the hexyl series. For example, for PS-DBPB57, the transition from smectic A to smectic C* on cooling is clearly marked by the appearance of helical pitch lines in the fans.

There are overall trends that were observed in the LC phase behavior of both block copolymer series as related to composition, molecular weight, and final block copolymer morphology. As can be seen from the data in Table 2, the liquid crystalline transition temperatures are affected by the length of the polystyrene block as well as the LC block. As the PS block is increased in MW, the cholesteric phase becomes narrower, and disappears at LC content at or below 43% (PS block length >10 000). For lower molecular weight samples, as the PS block length increases, the smectic A temperature range broadens at first, then appears to narrow at the longest PS lengths (32% LC). The smectic phases are apparently stabilized by the increased length of the PS block at the expense of the cholesteric phase; the smectic C* phase is particularly favored at higher molecular weights and longer PS chain lengths in these series. The stabilization effects of the smectic phases observed in simply increasing the size of the polystyrene block seem somewhat counterintuitive, as the morphology does not change for the samples studied and the

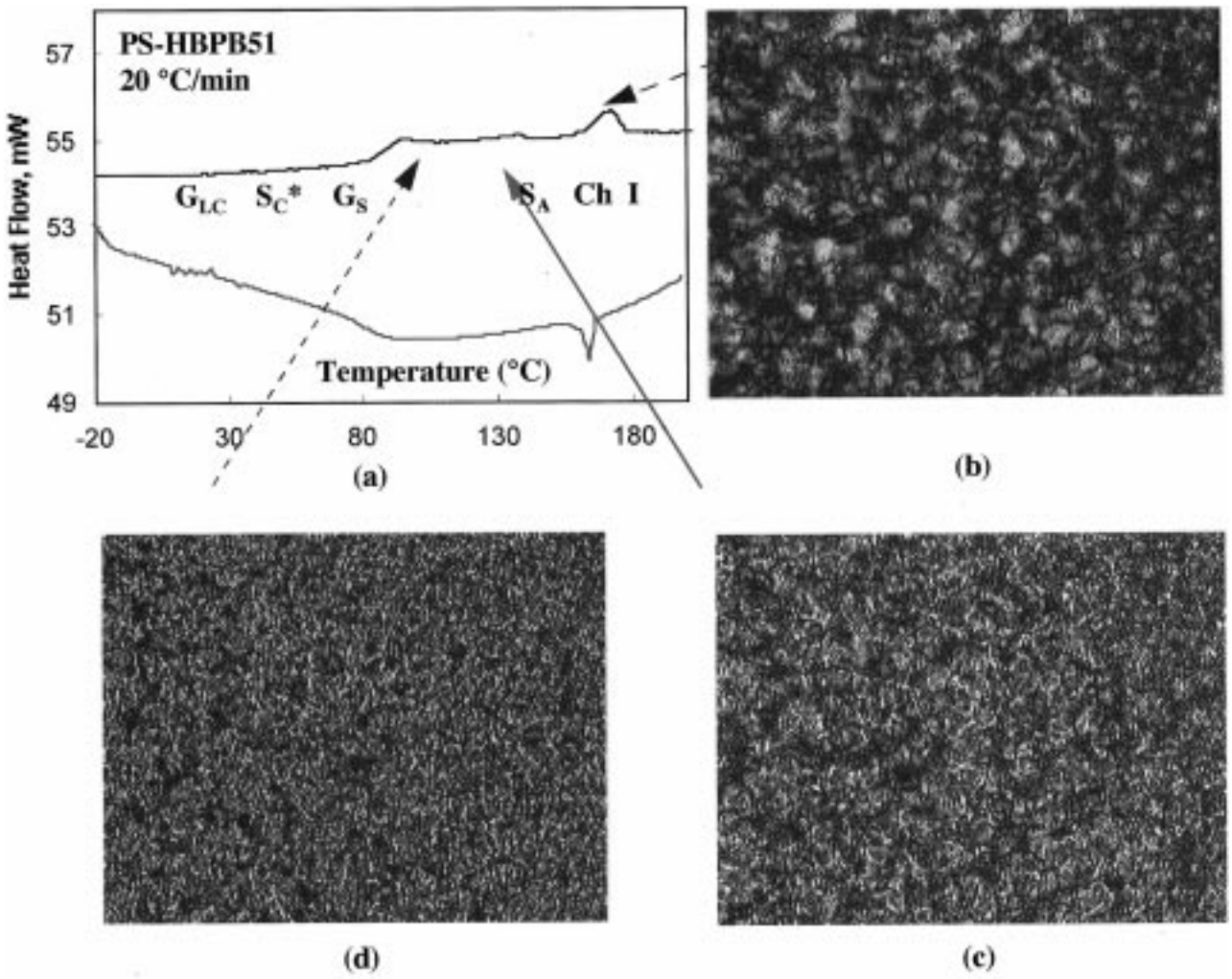

Figure 2. DSC thermogram (a) and corresponding LC textures for PS-HBPB51 block copolymer (b−d): (b) cholesteric texture at 167 °C; (c) S_A fine focal conic texture at 140 °C; (d) S_C* broken focal conic texture at 100 °C.

LC block domain does not change significantly in size. However, the degree of phase mixing changes considerably for longer PS lengths, particularly for the low overall molecular weight range considered here. Stabilization probably occurs as the result of the formation of a more well-defined block copolymer interface. The deviation of the polystyrene T_g from its pure value of 100 °C is due in part to phase mixing between the two blocks and to the varying length of the polystyrene segment. It is expected that higher molecular weights of the LC block will also increase the stability of the liquid crystalline phase; when the molecular weight of both the LC block and the PS block are increased, the clearing points are usually increased, as seen in PS-DBPB59 and PS-DBPB45.

The morphology of the block copolymer is expected to play a role in the LC transitions due to the presence of the block copolymer interface and any geometrical or confinement effects that interface may introduce. A detailed investigation of the block copolymer morphology will be presented in a separate paper;[16] however, it is relevant to mention the types of morphology observed here with respect to LC phase behavior. With very few exceptions, lamellar morphologies are exhibited by the block copolymers, as indicated in Table 2. In some samples with high LC content, as noted, defects typical of hexagonal perforated lamellar (HPL) or mixed layer morphology were sometimes observed; in these cases, lamellae were still the most often observed equilibrium morphology using TEM, particularly in oriented samples. We have found no indications of a cylindrical LC phase, implying that these materials have a tendency toward lamellar morphologies, perhaps due to the nature of the mesogen and the backbone. These observations are consistent with those made by Fischer et al.;[18,19] on the other hand, Mao et al. have observed smectic LC cylindrical morphologies with a polystyrene continuous phase for polyisoprene-based block copolymers.[12] The LC smectic phase stabilization observed here is apparently due to the presence of the block copolymer interface, which is particularly effective in stabilizing the smectic C* LC phase in the low molecular weight systems. At very high PS content, a morphology consisting of a liquid crystalline disperse phase in a polystyrene matrix results. For PS-HBPB24, only a weak birefringence was observed with no apparent diffraction peaks observed in WAXD, suggesting a weak nematic phase. No birefringent phase at all was observed in PS-HBPB20 and PS-HBPB12.

In this study we have found the lamellar block copolymer morphology to stabilize specifically the smectic LC phases. Stabilization effects of the smectic A phase were observed by Fischer et al.[19] in polystyrene−polymethacrylate cholesteryl based LC blocks. In this case, the smectic to isotropic clearing temperatures were found to increase from 125 to 200 °C with molecular

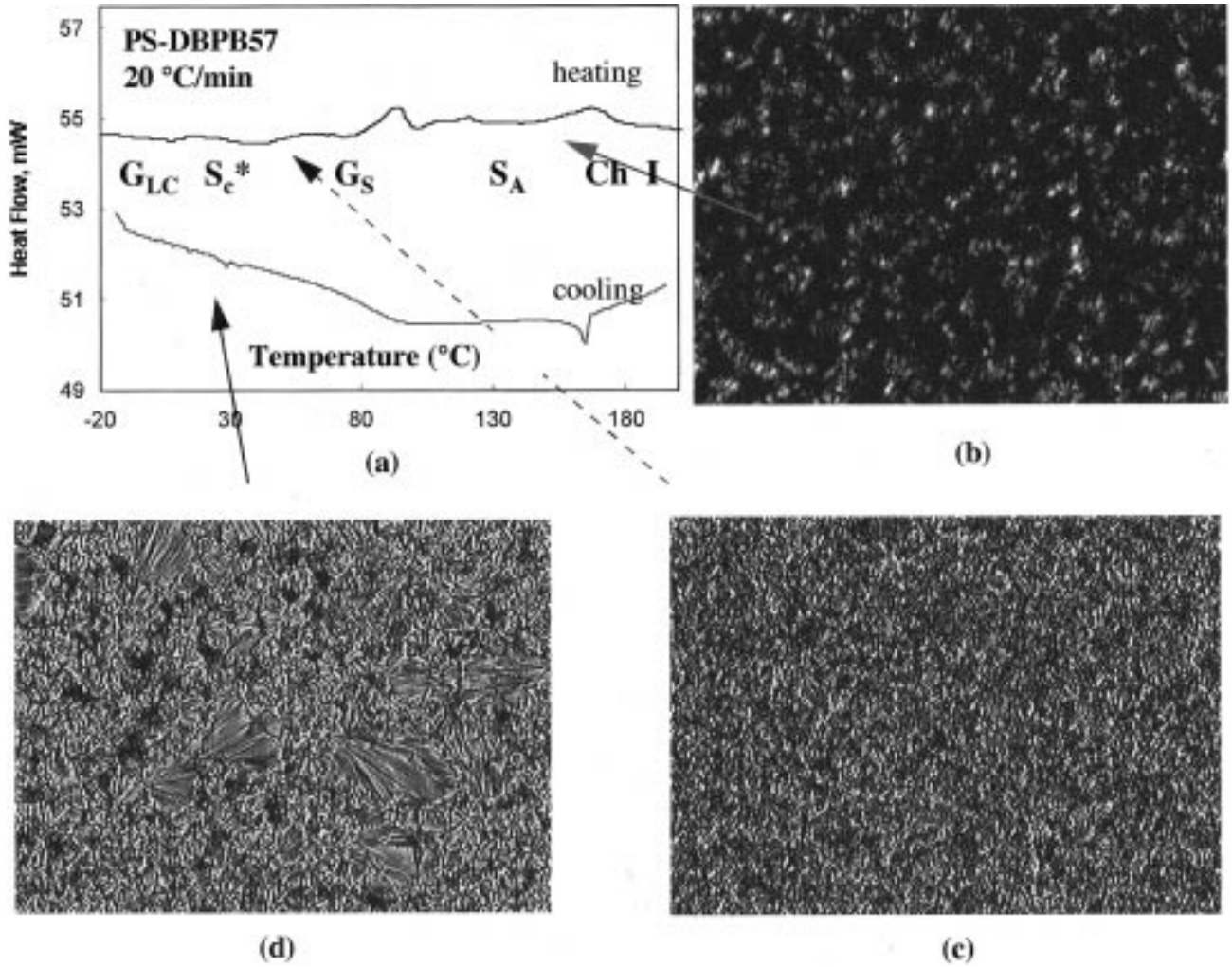

Figure 3. DSC thermogram (a) and corresponding LC textures for PS-DBPB57 Block Copolymer (b−d): (b) cholesteric phase near S_A transition, (c) schlieren texture of S_C* at 75 °C; (d) broken focal conic fans of S_C* at room temperature.

weight for the homopolymer, but to remain at 180 to 200 °C for all of the block copolymers, regardless of the MW of the smectic block. The stabilization seemed to be independent of the specific morphology of the block copolymer, suggesting that the general presence of block copolymer interface stabilizes the smectic phase. Sangar et al.[20] also found similar effects to those of Fischer. Bohnert and Finkelmann[17] did not find any stabilization effects due to block copolymer morphology; the block copolymers in this case were nematic and were apparently not as strongly influenced by the copolymer interface as the smectic phase. Recent reports on poly(vinyl ether) smectic block copolymers[21] actually indicate an inverse effect to the one reported here; the clearing points of the vinyl ether polymers decrease with increasing non-LC vinyl ether block content. It should be noted that a different weight composition range is probed in the Laus study, with LC content from 68 to 97% w/w. Phase morphologies were not described for these systems. In a study of azobenzene-functionalized block copolymers, Mao et al. discuss stabilization of the smectic phase for the cylindrical morphology but destabilization of the LC phase in the lamellar morphology.[12] The variations in findings suggest that stabilization of the smectic phase is due not only to the presence of the block copolymer interface but also to the compatibility of that interface with smectic layering, and the relative flexibility or chemical structure of the LC polymer backbone, which may influence factors such as the interfacial free energy at the interface and the ability of the backbone to accommodate smectic layering in confined spaces.

It is worth noting that the cholesteric phase exists in the block copolymers only at the lowest molecular weights, from 14 400 to 17 500, and at the highest liquid crystal compositions (PS-HBPB51, PS-DBPB63, and PS-DBPB57). Just as the lamellar structure of the block copolymers stabilizes the layered smectic phase, it apparently destabilizes the nematic phase. The nematic phase is also eliminated if the LC molecular weight is increased while maintaining constant LC block composition, as in the higher molecular weight copolymers PS-HBPB49 or PS-DBPB59. These results imply that the chiral nematic phase is not facilitated in the higher molecular weight polymers in general; these effects may be due to more effective phase segregation and well-defined lamellar interfaces and morphologies in the higher weight polymers. Domain size may also be an issue, as larger domains are able to better accommodate smectic LC arrangements. Finally, the block copolymers of the decyl series have clearing points considerably higher than the homopolymer, with an average increase of at least 20 °C in the LC block copolymers. The data in Table 2 suggest that the decyl series of polymers are even further stabilized by the presence of the glassy block than the hexyl series.

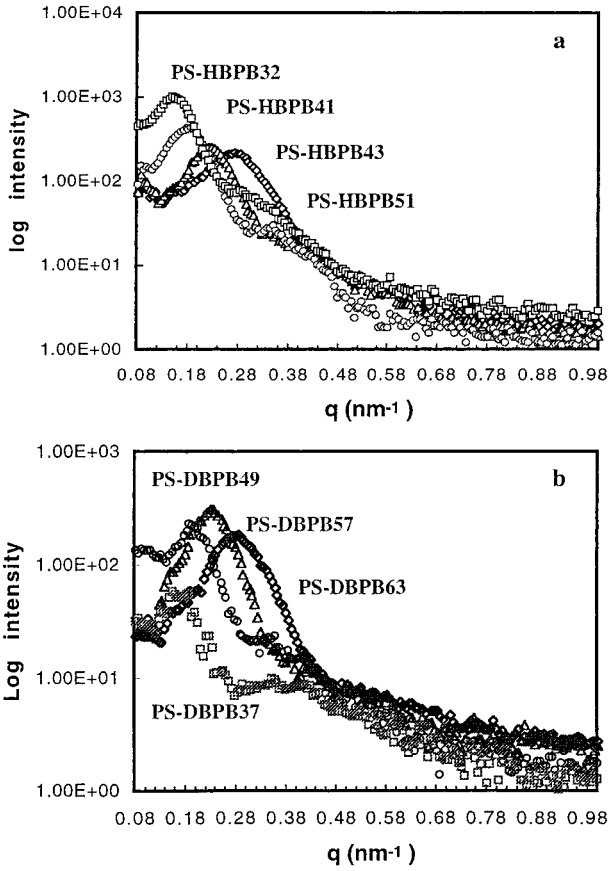

Figure 4. Room temperature SAXS profiles for each of the diblock copolymer series: (a) PS-HBPB series; (b) PS-DBPB series.

Table 3. List of SAXS *d*-Spacings for Hexyl and Decyl Block Copolymer Series

copolymer	$10^{-3}M_n$ (g/mol) diblock copolymer	SAXS *d*-spacing (nm)	morphology
PS-HBPB51	13.5	22.9	lamellar
PS-HBPB43	17.7	28.1	lamellar
PS-HBPB41	18.3	33.0	lamellar
PS-HBPB32	25.0	41.6	lamellar
PS-DBPB63	14.4	22.0	lamellar/HPL
PS-DBPB57	17.5	27.4	lamellar
PS-DBPB49	19.9	33.0	lamellar
PS-DBPB37	22.6	34.6	lamellar

Block Copolymer Phase Segregation and Domain Size. Small angle X-ray scattering was used to verify the presence of microphase segregation in the LC block copolymer series and to determine the associated domain size. SAXS profiles for each of the block copolymers are shown in parts a and b of Figure 4 for the hexyl and decyl series, respectively; the corresponding *d*-spacings of the block copolymers are given in Table 3. Phase morphology, when observed using TEM, is also reported here. All data were obtained from polymer cast film samples of roughly the same size and thickness, exposed to annealing at the designated temperature for several minutes before data were collected. From the SAXS data, we were able to determine the average *d*-spacings of the block copolymers, which ranged from 20 to 40 nm and increased with increasing length of the polystyrene chains, as expected. The polystyrene blocks were significantly larger than the liquid crystalline blocks. The average liquid crystalline segment in these polymers had approximately 20 repeat units. Polystyrene molecular weights varied from 6000 to 18 000, or from 60 to 180 repeat units. Despite the disparity in the lengths of these blocks, lamellar morphologies were observed using TEM techniques for most of the samples, as shown in the representative polymer sample in Figure 5. For the hexyl series of polymer, a peak in small angle was visible for samples with 32 wt % liquid crystal block and higher. No peaks were detectable using the available SAXS equipment for samples with 24% and lower LC content, although a diffuse morphology of disperse LC domains was observed in TEM for the 23% sample.

Figure 5. Representative lamellar morphology observed in TEM for LC block copolymer series. The sample shown is PS-HBPB32. Dark regions are polystyrene stained with RUO_4 and lighter regions are the LC copolymer.

The decyl spacer LC blocks are more compatible with the polystyrene blocks than was observed in the hexyl series polymers. For the lowest liquid crystal content polymer shown in Figure 4b, PS-DBPB37, the peak intensity is comparatively weak when compared to the other samples of similar thickness and higher LC content; the peak width in this sample is also greatly decreased, verifying the loss of scattering due to well phase segregated order. In this case, a lamellar morphology which was less well defined, with greater numbers of defects, was observed using TEM. This effect was not observed in the hexyl series polymers until much lower liquid crystal percentages (or larger polystyrene chain lengths) were reached. Thus it appears that the longer alkyl spacer acts to compatibilize the polystyrene and LC polymethacrylate blocks.

WAXD Studies. Wide angle X-ray diffraction was used to examine smectic LC order in the block copolymers and provided a means of monitoring LC phase transitions and a correlation between LC characteristic spacings and block copolymer morphology as temperature was varied. Figure 6 contains the WAXD diffractogram of an annealed film cast from toluene of PS-HBPB51 block copolymer at room temperature; an inset

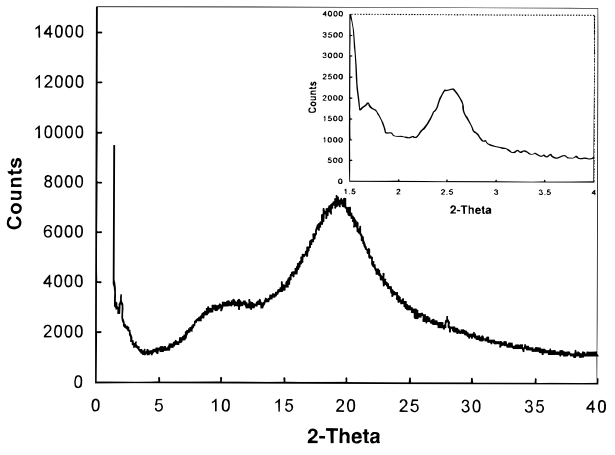

Figure 6. WAXD diffractogram of PS-BPB51 at room temperature. Inset shows detail of small angle region. Diffraction peaks due to smectic layers and to an *n*th order reflection of the block copolymer lamellae are shown.

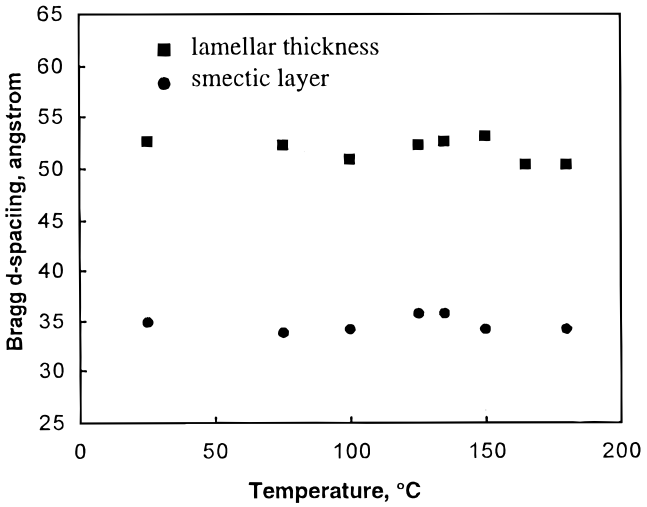

Figure 7. Plot of WAXD *d*-spacings versus temperature for smectic and lamellar peaks in annealed and quenched films of PS-HBPB51.

showing a detail of the small angle region is also given. WAXD data of the hexyl homopolymer has been reported previously. The smectic layer *d*-spacing corresponding to the small angle peak is 45 Å for the hexyl series homopolymer at 25 °C. As expected, the relative intensity of the smectic layer peak, when compared to the disordered amorphous halo in WAXD, is decreased for the block copolymer containing a polystyrene block versus the homopolymer. The peak is lowered in intensity considerably more than the weight fraction of 51% LC would suggest. This could be due to poor or incomplete ordering of the LC phase in the phase-segregated polymer sample. The block copolymer diffractogram exhibits two characteristic peaks that are within the range of the wide angle X-ray diffractometer; these are shown in the inset of Figure 6. When well-annealed films were used, higher order reflections due to the block copolymer lamellae spacing are visible in the diffractometer. For this reason, WAXD provides a convenient means of monitoring both forms of order in the block copolymers—the liquid crystalline and domain morphology ordering. The peak at the far left indicates a *d*-spacing of 52.5 Å. Comparisons with small angle X-ray data from a 2-D detector[16] indicate that this peak is the fourth-order reflection of the block copolymer lamellae. The peak at approximately 2.5° corresponds to the liquid crystal smectic layers and occurs at 34.9 Å. The relative heights of the two peaks change significantly with annealing; at long annealing times at 90 °C in films cast from toluene, the smectic layer peak becomes sharper and taller with respect to the reflection due to the lamellar domains. The liquid crystalline phase is not fully ordered in the as-cast films due to kinetics, and upon annealing at high temperature, a more perfectly ordered structure is obtained.

The positions of the lowest angle peaks in WAXD were monitored with temperature, as shown in Figure 7. Free standing film samples of the block copolymers were heated to a given temperature, annealed, and then quenched in ice water prior to WAXD experiments. As can be seen in Figure 7, there was a gradual increase in the *d*-spacing for the smectic layer from 33.7 Å at 75 °C to 35.7 Å as temperature was increased from the polystyrene glass transition up to 125 °C. This gradual increase is due to a decrease in the smectic tilt angle up to the smectic A phase. At 125−135 °C, the layer spacing levels off at 35.7 Å, presumably due to the smectic C to A transition, at which the maximum *d*-spacing is reached. Above 130 °C the *d*-spacing drops back down to 34 Å. It is characteristic of smectic A layer *d*-spacings to decrease gradually with temperature. At 180 °C, the smectic layer peak is still visible in the WAXD, but its intensity relative to the broad amorphous peak in the polymer diffractogram has decreased significantly, indicating the onset of loss of smectic ordering. The kinetic effects experienced when quenching to 0 °C prevented observation of complete loss of ordering in these samples.

The fourth-order reflection peak of the block copolymer lamellar domains was also monitored in the WAXD with temperature increase. The domain spacing appears to remain fairly constant at low temperatures; however, above 100 °C, which is the glass transition temperature of polystyrene, there is a gradual increase in the lamellar spacing that is coincident with smectic layer thickness increases as the smectic C* tilt angle approaches zero. The increased mobility of the block copolymer above the T_g may allow changes in the lamellae dimensions that best suit the arrangement of the smectic layers. The increase is followed by a sharp drop in spacing. This change in spacing coincides roughly with the onset of the nematic phase at 167 °C and the clearing point at 170 °C. The drop in spacing is probably due to the loss of the physical constraint that the smectic layer phase arrangement places on the LC block dimensions as it goes from the LC to the disordered state. The dimensional change is a result of a more random arrangement of the polymer backbone and side chains. Watanabe observed decreases in the block copolymer lamellar spacings of an LC block copolymer based on a methacrylate backbone when the LC block transitioned from a crystalline to a smectic A phase.[7] In the Watanabe study, the LC backbone is fairly extended in the crystalline state and is thought to approach a more random coil arrangement in the smectic A phase; as the isotropic phase is entered, the *d*-spacing levels off, with an overall decrease in *d*-spacing of 50 Å. In comparison, the dimensional changes observed in the BPB series are much more moderate, though it is clear that the block copolymer lamellar spacing mimics the changes observed in the LC smectic layer. Apparently, the smectic layer thickness directly affects the thickness of the block copolymer lamellae.

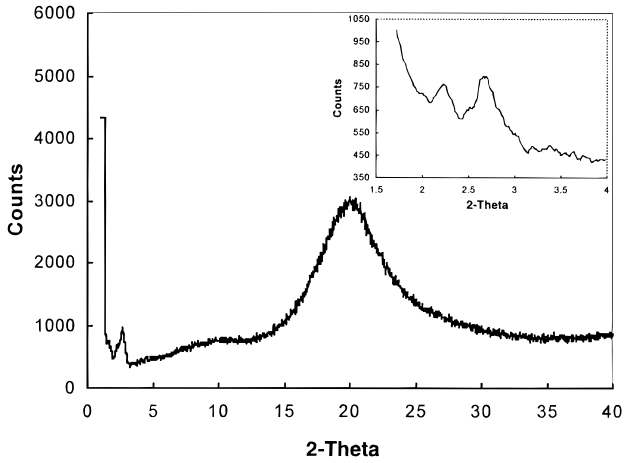

Figure 8. WAXD diffractogram of PS-DBPB59 at room temperature. Inset shows detail of small angle region.

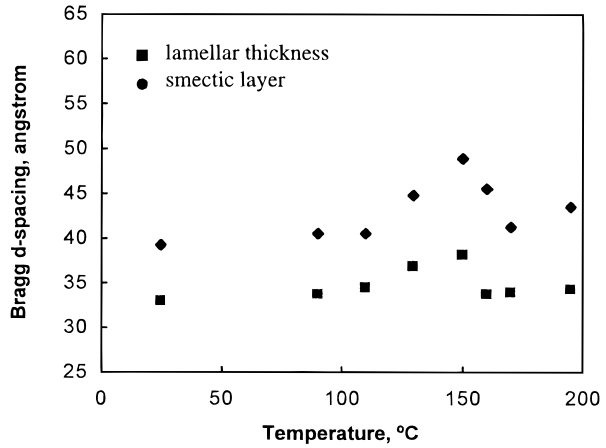

Figure 9. Plot of WAXD *d*-spacings versus temperature for smectic and lamellar peaks in annealed and quenched films of PS-DBPB59.

The decyl block copolymer, PS-DBPB59, exhibits a similar smectic WAXD diffractogram, as shown in Figure 8. In this case, the smectic layer has a first-order reflection at 32 Å and a peak due to the higher order reflection of the lamellar blocks at 39 Å. In the sample shown, the smectic peak is fairly weak, perhaps due to incomplete ordering during annealing; at higher temperatures, the smectic peak becomes sharper and more well-defined. Figure 9 contains a plot of *d*-spacing versus temperature for PS-DBPB59. As temperature is increased in the smectic C* phase, a monotonic increase in the *d*-spacing of the smectic layer is observed from 32 to 38 Å, an indication of the transition from the tilted smectic C* to smectic A phase at 150 °C. The transition temperature is close to values observed in the polymer using the DSC in first and second heatings; the value observed is higher, probably due to kinetic effects in the quenching experiment. It is interesting to note that an apparent slope change is observed in the plot at 100 °C, just above the glass transition temperature of the polystyrene block. The increased mobility of the block copolymer at the glass transition of polystyrene may enable the movement and tilt of the smectic mesogen. At temperatures above 150 °C, there is a drop in the *d*-spacing down to 34 Å. The kinetic effects of the quenching experiment prevented the observation of the clearing point, and a smectic peak was observed even when the sample was quenched from 195 °C. As was observed in the hexyl series of block copolymers, the PS-DBPB59

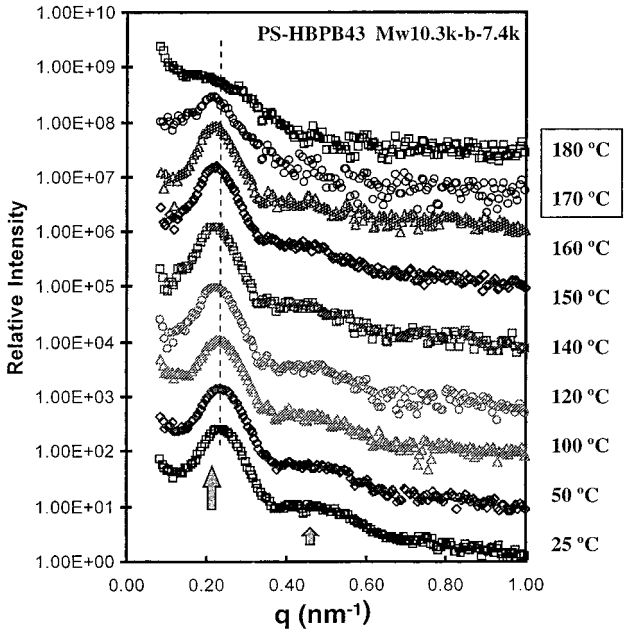

Figure 10. SAXS profiles of PS-HBPB41 at elevated temperatures.

block copolymer lamellae also undergo very similar changes in *d*-spacing when compared with the smectic layers, as shown in Figure 9. In this case, the domains appear to expand in size with temperatures above the polystyrene glass transition in a monotonic manner up to 150 °C, at which a drop in spacing is observed.

LC Block Copolymers and the ODT Transition. SAXS temperature studies were performed in-situ using a Mettler hotstage in the SAXS detector. Scattering profiles with temperature are shown in Figure 10 for PS-HBPB43, a block copolymer typical of this series, with an overall molecular weight of approximately 18 000. In this experiment, the same block copolymer sample film is examined using SAXS in situ with a hot stage at varying temperatures. As the temperature is increased, the broad small angle peak signifying a phase-segregated morphology broadens and disappears between 170 and 180 °C. At this temperature, the peak originally present in the sample at lower temperatures is barely discernible. This rapid drop in scattering is associated with the loss of strong phase segregation in the block copolymer, and signifies an order−disorder transition (ODT) from a microphase segregated to a phase mixed block copolymer. The isotropization temperature of the liquid crystalline phase for this polymer is 176 °C, in the same range that the ODT is observed. Apparently, microphase segregation is induced by the introduction of liquid crystalline ordering. These results are the first to suggest the dependence of the ODT on the LC clearing point for LC block copolymers. This dependency suggests that liquid crystal formation is actually the thermodynamic driving force for microphase segregation for this system.

When a similar experiment was conducted with PS-HBPB32 (Figure 11), which has a slightly higher molecular weight of 25 000 due to the increased length of the polystyrene block, the order−disorder transition no longer occurs at the LC clearing point. The SAXS peak remains present at approximately the same intensity throughout the range of temperatures used in the experiment. At higher molecular weights, the value of χN is larger, and the driving force for microphase

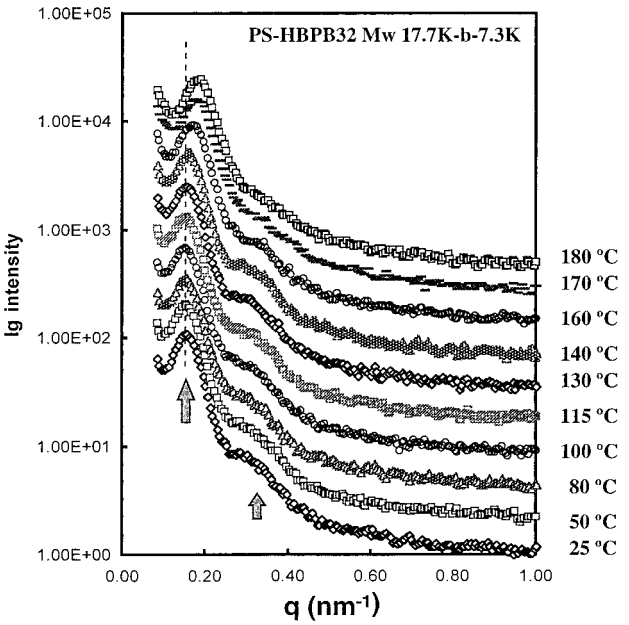

Figure 11. SAXS profiles of PS-HBPB32 at elevated temperatures.

segregation is sufficient for block copolymer domain morphology to exist at temperatures above that of the liquid crystalline phase. What is interesting about the SAXS data in Figure 11 is that the location of the SAXS peak shifts to lower *d*-spacings at the temperature corresponding to the liquid crystalline clearing point and the second-order reflection becomes noticeably diminished. This is an indication that the rearrangements of the mesogen within the block copolymer domains are such that the domains are slightly expanded to accommodate the mesophase smectic layers, as observed with WAXD measurements. On clearing, the random conformation of the LC block is approached, and the domains get smaller with respect to the expanded state in the LC.

The SAXS data provide us with a picture of the role of the mesophase in the formation of phase-segregated morphologies. To describe this effect, we can take the basic set of criteria for microphase segregation, with a slight modification for the LC phase:

Microphase segregation occurs when

$$\chi_{\text{eff}} N > (\chi_{\text{eff}} N)_{\text{crit}}$$

$$\chi_{\text{eff}} = \chi + \chi_{\text{LC}}$$

where χ is the Flory Huggins parameter between the polystyrene and polymethacrylate blocks based on intermolecular interactions between the two polymer blocks in the isotropic melt, N is the molecular weight, and we modify the Flory−Huggins parameter to account for liquid crystalline order with an effective chi parameter, χ_{eff}. We can expect the effect of LC order in the system to greatly reduce the interactions between the ordered and the disordered block and thus increase χ_{eff}. Therefore, we can assume a positive contribution, χ_{LC}, which is added to the value of χ_{eff} on cooling below the isotropic state. If the overall value of χN, based on polymer segmental interactions alone, is just below the critical value required for phase segregation, the introduction of liquid crystallinity at the isotropic−LC transition is enough to induce phase segregation. If, however, χN is larger than the critical value above the clearing point, phase-segregated morphology will already exist, and the liquid crystalline order, when introduced, must be formed within existing phase-segregated domains.

In the first case, in which liquid crystalline order induces the phase segregation of the block copolymer, we might expect to see the block copolymer morphology

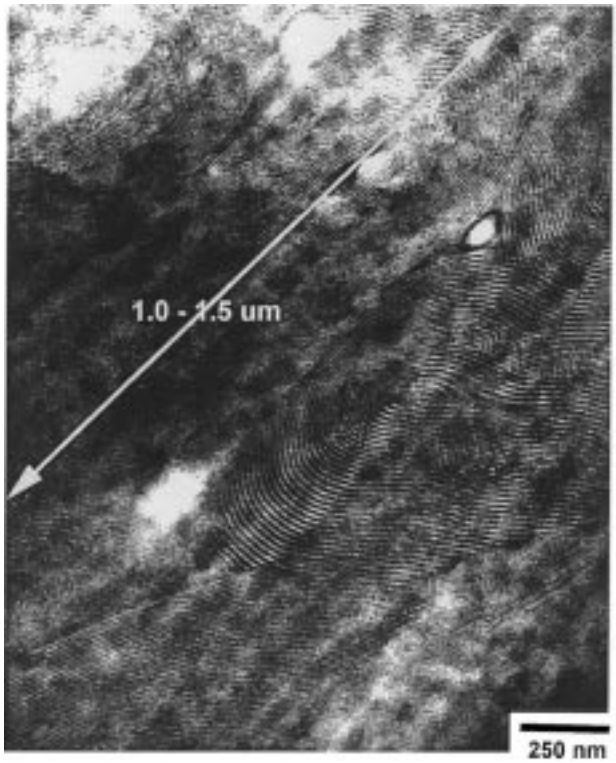

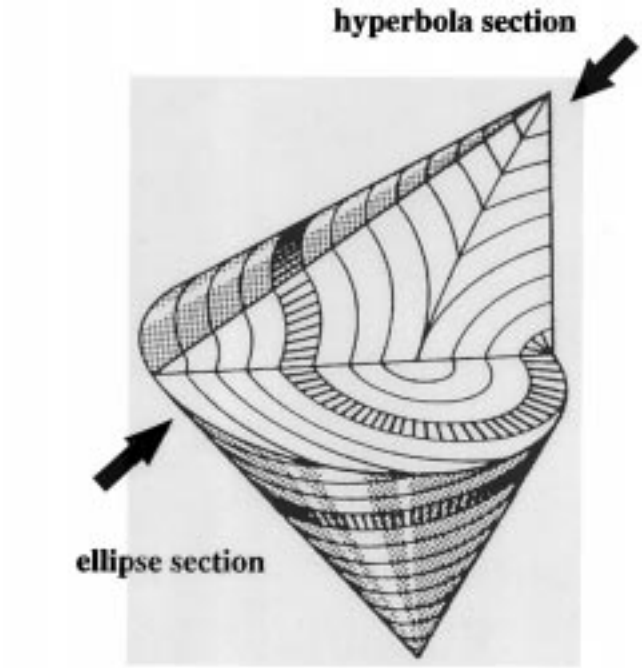

Figure 12. (a) Onion-like morphology reminiscent of Dupin cyclides in annealed samples of PS-DBPB63. Dark regions are the polystyrene domains. (b) Classical focal conic domain superstructure for smectic liquid crystals (adapted from Gray and Goodby[25]).

strongly influenced by liquid crystalline texture. There is some evidence of such an influence in the highest LC content polymers of this series. A TEM micrograph of PSDBPB63 is shown in Figure 12a. Here the polystyrene regions appear dark due to the RuO_4 stain. The curved lamellae exist in onion-shaped superstructures that range in size from about 0.25 to several micrometers. These shapes are reminiscent of focal conic arrangements seen in typical smectic liquid crystals, illustrated in Figure 12b; we have found these structures thus far in LC block copolymer systems which have a large LC content and low molecular weight, often the same samples that have an LC-induced ODT. Although curvy lamellae are common in block copolymers, well-defined cyclides such as these are not very commonly observed. It appears that the polystyrene blocks are actually incorporated into the liquid crystal superstructure in these polymers, producing micrometer-sized focal conic fans.

Semicrystalline block copolymers provide an ideal analogy to the observed order-induced ODT behavior described here. Cohen et al.[22] found that the morphology of polystyrene-hydrogenated butadiene block copolymers were very dependent on the temperature used for annealing or for solvent removal. In cases in which crystallites began to form before microphase segregation, a spherulitic texture was formed, with virtually undiscernible block copolymer domains. When annealed above the melt temperature, the expected spherical morphology was observed. Register et al. found that crystallization was the driving force for phase segregation in poly(ethylene/ethylene−propylene) block copolymers using time-resolved SAXS studies.[23] The semicrystalline diblocks were shown to exhibit lamellar morphologies at fairly low fractions of polystyrene, with a spherulitic superstructure typical of semicrystalline homopolymers,[24] just as a focal conic structure is found in some of the BPB block copolymers. Thus far, there have been no reports of the link between ODT, morphological superstructure, and LC phase behavior. The superposition of order is dependent on the molecular weight and composition but is also dependent on the relative size of χ, i.e., the incompatibility between the two blocks. These factors explain why this behavior may not have been observed in previous studies of side chain LC block copolymers. We are currently studying the morphologies of these block copolymers in great depth, including SAXS and TEM of oriented samples. A separate paper on morphological behavior will be used to report those results.

Conclusions

The liquid crystalline and morphological phase behavior of a new series of polystyrene−polymethacrylate smectic C* side chain liquid crystalline block copolymers represents a superposition of LC and microphase segregated order. The lamellar block copolymers appear to stabilize the smectic C* phase over the smectic A and nematic liquid crystalline phases. For lower molecular weight polymers, the degree of stabilization is even more significant when compared to homopolymer of similar molecular weight. On the other hand, the presence of a layered smectic phase resulted in block copolymers with lamellar morphologies at fairly asymmetric compositions, when the LC block was the minority fraction. In short, it appears that lamellar arrangements in the smectic LC and the block copolymer effectively stabilize each other.

The order−disorder transition temperature of LC block copolymers in this series of low molecular weights coincided with the LC clearing point; as liquid crystalline order developed in the samples, microphase segregation took place. The appearance of LC order at or before the development of block copolymer domains in these cases results in annealed superstructures which appear to be focal conic. The influence of mesophase order on morphology is dependent on the molecular weight and compatibility between the polymer blocks and can be discussed with respect to an additional contribution to the Flory−Huggins parameter due to liquid crystal ordering. The phase morphology is greatly influenced by the LC block, which indicates the strong effect even low molecular weight blocks can have on the final properties of the block copolymer. The fact that LC ordering can be used to trigger the ODT and influence morphology in certain block copolymers presents interesting possibilities for the development of smart or responsive materials, as well as electro-optical systems, and provides a key to further understanding the cooperativity of liquid crystalline and microphase segregated order.

Acknowledgment. The authors gratefully acknowledge the National Science Foundation Polymer Program for funding under Grant Number DMR-9526394. This work was also supported by the MIT Center for Materials Science and Engineering DMR-9400334. P. Hammond gratefully thanks the DuPont Corporation for its support through the DuPont Young Faculty Award. Special acknowledgments are given to David Wall and Thomas Epps of the Massachusetts Institute of Technology, Department of Chemical Engineering. We also thank Professor Ned Thomas for use of his ultracryomicrotome equipment and to Professor Bob Cohen for the use of his SAXS facility.

References and Notes

(1) Adams, J.; Gronski, W. *Makromol. Chem., Rapid Commun.* **1989**, *10*, 553−557.
(2) Zaschke, B.; Frank, W.; Fischer, H.; Schmutzler, K.; Arnold, M. *Polym. Bull.* **1991**, *27*, 1−8.
(3) Hefft, M.; Springer, J. *Macromol. Chem., Rapid Commun.* **1990**, *11*, 397.
(4) Percec, V.; Lee, M. *J. Macromol. Sci., Chem.* **1992**, *29*, 723.
(5) Komiya, Z.; Schrock, R. R. *Macromolecules* **1993**, *26*, 1387.
(6) Chiellini, E.; Galli, G.; Angeloni, A. S.; Laus, M.; Bignozzi, M. C. *Macromol. Symp.* **1994**, *77*, 349−358.
(7) Yamada, M.; Iguchi, T.; Hirao, A.; Nakahama, S.; Watanabe, J. *Macromolecules* **1995**, *28*, 50−58.
(8) Chen, J. T.; Thomas, E. L.; Ober, C. K.; Mao, G. *Science* **1996**, *273*, 343.
(9) Zheng, W. Y.; Hammond, P. T. *Macromol. Rapid Commun.* **1996**, *17*, 813−824.
(10) Zheng, W. Y.; Hammond, P. T. Side Chain Liquid Crystalline Block Copolymers with Chiral Smectic C Mesogens. In *Liquid Crystals for Advanced Technologies*; Chen, S. H., Bunning, T. J., Hawthorne, W., Koide, N., Kajiyama, T. Eds.; MRS Symposium Proceedings: San Francisco, CA, 1996; Vol. 425.
(11) Omenat, A.; Hikmet, R. A. M.; Lub, J.; van der Sluis, P. *Macromolecules* **1996**, *29*, 6730−6736.
(12) Mao, G.; Wang, J.; Clingman, S. R.; Ober, K.; Chen, J. T.; Thomas, E. L. *Macromolecules* **1997**, *30*, 2556−2567.
(13) Chiellini, E.; Galli, G.; Angeloni, S.; Laus, M. *Modern Trends Polym. Sci.* **1994**, *2*, 244.
(14) Zheng, W. Y.; Hammond, P. T. Synthesis and Characterization of Block Copolymers with Smectic C* Liquid Crystalline Mesogens. Presented at the AIChE Annual Meeting, Miami, November 1995.
(15) Mao, G.; Wang, J.; Ober, C. K.; O'Rourke, M. J.; Thomas, E. L.; Brehmer, M.; Zentel, R. *Polym. Prepr.* **1997**, *38*, 374−375.

(16) Zheng, W. Y.; Hammond, P. To be submitted to *Macromolecules*.
(17) Bohnert, R.; Finkelmann, H. *Macromol. Chem. Phys.* **1994**, *195*, 689−700.
(18) Fischer, H.; Poser, S.; Arnold, M.; Frank, W. *Macromolecules* **1994**, *27*, 7133−7138.
(19) Fischer, H.; Poser, S.; Arnold, M. *Liq. Cryst.* **1995**, *18*, 503−509.
(20) Sangar, J.; Tefehne, J.; Gronski, W. *Macromol. Rapid Commun.* **1994**, *15*, 879.
(21) Laus, M.; Bignozzi, M. C.; Fagnani, M.; Angeloni, A. S. *Macromolecules* **1996**, *29*, 5111−5118.
(22) Cohen, R. E.; Cheng, P. L.; Douzinas, K.; Kofinas, P.; Berney, C. V. *Macromolecules* **1990**, *23*, 324−327.
(23) Rangarajan, P.; Register, R.; Adamson, D. H.; Fetters, L. J.; Bras, W.; Naylor, S.; Ryan, A. J. *Macromolecules* **1995**, *28*, 1422−1428.
(24) Rangarajan, P.; Register, R.; Fetters, L. J. *Macromolecules* **1993**, *26*, 4640−4645.
(25) Gray, G. W.; Goodby, J. W. G. *Smectic Liquid Crystals*; Heydon and Son, Inc.: Philadelphia, PA, 1984.

MA970940C